Chalcogenide Letters Vol. 8, No. 5, May 2011, p. 355 - 361

STRUCTURAL STUDY OF SILVER PHOTODOPED Ge-Sb-Te FILMS

SANDEEP KUMAR, DIGVIJAY SINGH, R. THANGARAJ*
Semiconductors Laboratory, Department of Physics, Guru Nanak Dev University, Amritsar-143005, India

We have investigated silver diffusion driven by irradiation with light in Ge-Sb-Te amorphous thin films close to the composition $Ge_{22}Sb_{22}Te_{56}$. X-ray diffraction studies indicate that, after Ag photodoping, $Ge_{22}Sb_{22}Te_{56}$ film remains amorphous. Quantitative data regarding the composition of Ge-Sb-Te amorphous thin film and amount of photodoped silver has been gathered using electron probe micro-analyzer (EPMA) having wavelength dispersive spectroscopy (WDS). The actual composition of the film was found to be $Ge_{23}Sb_{23}Te_{54}$ and amount of silver photodoped was ~ 2.5 at. % in the glassy matrix. The qualitative analysis of $Ge_{23}Sb_{23}Te_{54}$ film and Ag-photodoped $(Ge_{23}Sb_{23}Te_{54})_{100-x}Ag_{x=2.5}$films was done with x-ray photoelectron spectroscopy (XPS). The XPS data consisted of survey scans from the binding energy ranging from 0 to 700 eV and selected scans over the valence band peaks of interest (Ge 3d, Te 3d, Sb 3d and 4d, and Ag 3d). Chemical shift of constituent elements revealed that electrons are transferred from chalcogenide to metal and compounds such as Ag_2Te are likely to be formed due to photo induced changes. The structure of annealed films was studied with x-ray diffraction and temperature dependent sheet resistance measurements.

(Received April 21, 2011; Accepted May 27, 2011)

Keywords: Amorphous chalcogenides; Thin films; Photodoping

1. Introduction

The migration of various metals (pre-dominantly, Ag, Cu, Zn) in amorphous chalcogenides under exposure of light has been studied for many years [1-4]. This effect is a characteristic of chalcogenide amorphous semiconductors when metals are deposited on films of these materials. Diffusion of metal into the film occurs by means of light irradiation mainly visible (near bandgap) light. The effect has been long ago demonstrated [5] and terms such as photodiffusion, photodoping, and photodissolution have been used over the years [3]. The incorporation of appreciable amounts of a metal in the chalcogenide material alters the composition and hence the structure and the physicochemical properties of the material. Obviously, the most affected properties are the optical properties that can be exploited in a number of advanced technological applications, e.g., in optoelectronics (diffraction gratings, photonic bandgap structures, resists for nanolithography, etc.) [2]. Photodiffusion is one such process, where one can introduce high concentration of dopant into glassy matrix [6]. It is found that GeSbTe alloys are particularly well suited for satisfying all the requirements associated with data storage applications. The pronounced difference in the optical properties leads to high contrast, which is one of the attractive features of phase change recording [7]. From GeSbTe alloy, four different types of compositions $Ge_2Sb_2Te_5$, $Ge_1Sb_4Te_7$, $Ge_1Sb_2Te_4$, and $Ge_4Sb_1Te_5$, formed along the GeTe-Sb_2Te_3 tie line, have been identified. Among them, most studies have focused on $Ge_2Sb_2Te_5$ (GST) due to its excellent properties with respect to achievability, reflectivity contrast, cyclability, and crystallization speed [8]. Nevertheless, for the further development of data storage media both storage densities and data transfer rates need to be increased. Doping is the most

*Corresponding author: rthangaraj@rediffmail.com; semi.vacuum@gmail.com

effective method to improve the properties of phase change materials. Recently, elements such as Ag, Bi, Al etc. have been doped into Ge-Sb-Te films [8-10]. But photodoping of metal impurity in Ge-Sb-Te alloy films are still not studied well. The aim of present work is to investigate the Ag-photodoping in $Ge_{22}Sb_{22}Te_{56}$ amorphous thin films and characterize them with various techniques (EPMA, XPS and XRD). The structural analysis of annealed films was done with x-ray diffraction studies and sheet resistance measurements.

2. Experimental

The alloy of $Ge_{22}Sb_{22}Te_{56}$ was synthesized using 99.999% elemental Ge, Sb and Te sealed in quartz ampoule (length ~10 cm, internal diameter ~6 mm) evacuated to ~10^{-5} mbar. The melt was homogenized at 1000 ^{o}C, at a rate of 4-5 ^{o}C/min for at least 48 h and finally cooled. Cooling was done by switching off the furnace leaving ampoule inside. Ampoule was taken out of the furnace at room temperature and broken carefully to extract the sample. Peaks of $Ge_2Sb_2Te_5$ (GST) were identified in the x-ray scan of above prepared alloy. Using this source alloy, amorphous thin films of approximately 200 nm were prepared by thermal evaporation method using Hind High Vacuum Coating Unit (Model No. 12A4D). Well cleaned glass slides were used as substrates and molybdenum boats containing the source material were used for the deposition. The substrates were maintained at room temperature during the deposition and the pressure in the chamber during the deposition was below 10^{-5} mbar. The films were left inside the chamber for ~24 h to attain metastable equilibrium as-suggested by Abkowitz [11]. The actual composition of the deposited films was determined by electron probe micro-analyzer (EPMA) as $Ge_{23}Sb_{23}Te_{54.}$ A silver film ~20 nm was evaporated on the top of the previously grown amorphous films to form Ag:Ge-Sb-Te bilayer.

The photodiffusion was performed using illumination of the film with halogen lamp (Halonix 500W) from silver side in Ag:Ge-Sb-Te bilayer for 20 min. at room temperature in inert atmosphere. After the diffusion processes were complete, the remnant Ag on the film surface was dissolved in 0.1N solution of $Fe(NO_3)_3$ [12]. The amount of diffused Ag was determined by means of EPMA (CAMECA SX 100) analysis using 15 KeV electrons with beam size 10 μm, the sample current was 20 nA and samples were coated with very thin film of carbon in vacuum chamber before EPMA analysis. The wavelength dispersive spectroscopy (WDS) was used for the compositional measurements. It is found that 2.5 at. % of Ag has been diffused in the glassy matrix. X-ray photoelectron spectroscopy (XPS) was carried out to examine the chemical environment and product that form after the Ag diffusion into $Ge_{23}Sb_{23}Te_{54}$ films. The x-ray photoelectron spectrum was recorded in an ESCA instrument (VSW) using Al K_{α} radiation at 2X 10^{-9} torr base vacuum. To remove surface contamination the samples were sputtered with Ar^{+} ions with energy of 0.5 KeV and current density of Ar^{+} approximately 10 μA/cm^2 having pit size 1cm^2. The crystal structure of bulk alloy, as-deposited $Ge_{23}Sb_{23}Te_{54}$, photodoped $(Ge_{23}Sb_{23}Te_{54})_{100-x}Ag_{x=2.5}$films and the annealed films were identified by using Cu-K_{α} lines of x-ray-diffraction studies. A change in sheet resistance as a function of annealing temperature and amorphous-crystalline transformation temperatures of the samples were measured with a two-point probe. The sheet resistance measurements were done in vacuum chamber having pressure ~10^{-4} mbar and the values were averaged after three time measurements. The temperature at which an abrupt drop in the resistance takes place was taken as amorphous-crystalline phase transformation temperature.

3. Results and discussion

3.1. *Electron probe micro-analyzer (EPMA)*

The composition of as-deposited $Ge_{22}Sb_{22}Te_{56}$ and Ag-photodoped $Ge_{22}Sb_{22}Te_{56}$ films are determined by electron probe micro-analyzer (EPMA). Table 1 shows the atomic percentage of all the elements present in the films. From the table, it is observed that the composition of films is

$Ge_{23}Sb_{23}Te_{54}$ approximately same as the initial composition taken for the preparation of bulk material and amount of Ag photodoped is ~ 2.5 at. % in the $Ge_{23}Sb_{23}Te_{54}$ amorphous films.

Table 1. The at. % of Ge, Sb, Te and Ag in undoped and photodoped samples calculated from EPMA data.

Samples with initial composition	Elements	Atomic %				Samples with actual composition
		Spot 1	Spot 2	Spot 3	Average	
As-deposited $Ge_{22}Sb_{22}Te_{56}$	Ge	23.1	22.9	23.0	23.0	$(Ge_{23}Sb_{23}Te_{54})_{100-x}Ag_{x=0}$
	Sb	23.1	22.8	22.7	22.8	
	Te	53.9	54.3	54.3	54.2	
Ag-photodoped $Ge_{22}Sb_{22}Te_{56}$	Ge	22.1	22.6	22.8	22.5	$(Ge_{23}Sb_{23}Te_{54})_{100-x}Ag_{x=2.5}$
	Sb	22.4	22.9	22.6	22.6	
	Te	53.1	51.9	52.1	52.5	
	Ag	2.4	2.5	2.5	2.5	

3.2. X-ray photoelectron spectroscopy

X-ray photoelectron spectroscopy (XPS) is a surface sensitive technique with about 65% of the signal obtaining from the outermost ~ 3 nm of the film [13]. Fig. 1 shows the survey scan of as-deposited $Ge_{23}Sb_{23}Te_{54}$ and Ag-photodoped $(Ge_{23}Sb_{23}Te_{54})_{100-x}Ag_{x=2.5}$films from binding energy 0 to 700 eV. The satisfactory level of the signals for Ge, Sb, Te and Ag is obtained in the survey scan. The films are contaminated with O during transportation of the films from deposition devise to the XPS analysis chamber. As binding energies of the O 1s (531.8eV) peak and Sb 3d (528.2eV) peak are approximate same so we cannot found separate signal of O 1s peak. Furthermore, C 1s can be detected due to surface contamination with hydrocarbon after transportation in air.

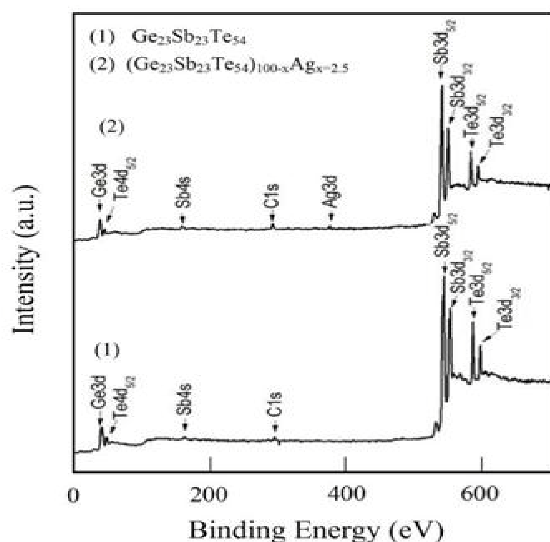

Fig. 1. XPS survey scan (1) $Ge_{23}Sb_{23}Te_{54}$ as-deposited and (2) photodoped $(Ge_{23}Sb_{23}Te_{54})_{100-x}Ag_{x=2.5}$ films.

Fig. 2, Fig. 3 shows the XPS spectra of Ag-photodoped $(Ge_{23}Sb_{23}Te_{54})_{100-x}Ag_{x=2.5}$ amorphous films. According to the XPS results, Ge 3d (binding energy: 32.6 eV), Sb 3d and 4d (binding energy: 531.1 eV, 540.3 eV and 34.5 eV respectively) (Figure 2) and Te (binding energy: 573.0 eV and 583.4 eV) (Figure 3) are forming a part of Ge-Sb-Te (GST) alloy. The position of Ge, Sb and Te peaks are in good agreement with value reported in the literature for the pure

$Ge_2Sb_2Te_5$ films. Core level spectra of Ag 3d (binding energy: 268.6 eV) is higher than the binding energy of elemental Ag (Figure 2 b). We used the C 1s peak at 285.0 eV to calibrate the experimental results. From the XPS handbook, the binding energy of Ge-Ge and Ge-O are approximately 29.7 eV and 31.4 eV for Ge 3d core level peak respectively [14]. There is no peak at about 29.7 eV related to the Ge-Ge homopolar bond in figure 2 (a), denoting that the Ge atom do not have a homopolar Ge-Ge bond but rather a bond with Sb or Te in amorphous Ge-Sb-Te glassy matrix of thin films. However, the fact that GeTe alloy has a Ge-Ge bond suggest that the addition of Sb atom prevent the formation of Ge-Ge bonds [15]. The peak positions of Sb 3d are shown in Fig. 2 (b) with binding energies of homopolar Sb-Sb bonds approximately 528 eV and 537.4 eV and Sb-O bonds approximately 531.1 eV and 540.3 eV for Sb $3d_{5/2}$ and Sb $3d_{3/2}$ respectively [14]. The fact that there is no peaks related to Sb-Sb bonds and there are Sb-metallic bonds indicates that Sb atoms, like Ge, have Sb-Ge or Sb-Te bonds rather than Sb-Sb bonds. However, in case of Te, there is Te-Te chain with in the Te $3d_{3/2}$ peaks, with binding energy of 583.4 eV indicating that along Te-metallic bond include the homopolar Te bond [14] and small negative binding energy shift of 0.3 eV in Te $3d_{3/2}$ is due to Te-metallic bond probably Te-Ag. The binding energy of Te-Te $3d_{3/2}$ is 572.8 eV [14]. Figure 2(d) is XPS scan for Ag 3d core level peak of the Ag-photodoped $(Ge_{23}Sb_{23}Te_{54})_{100-x}Ag_{x=2.5}$ film indicates the chemical shift 0.5 eV for $3d_{3/2}$ and $3d_{5/2}$ higher than in case of pure silver (368.2 eV). This strongly suggest that Ag in the glass matrix is not in the elemental form and there is considerable formation of Ag-Te bond probably Ag_2Te [12].

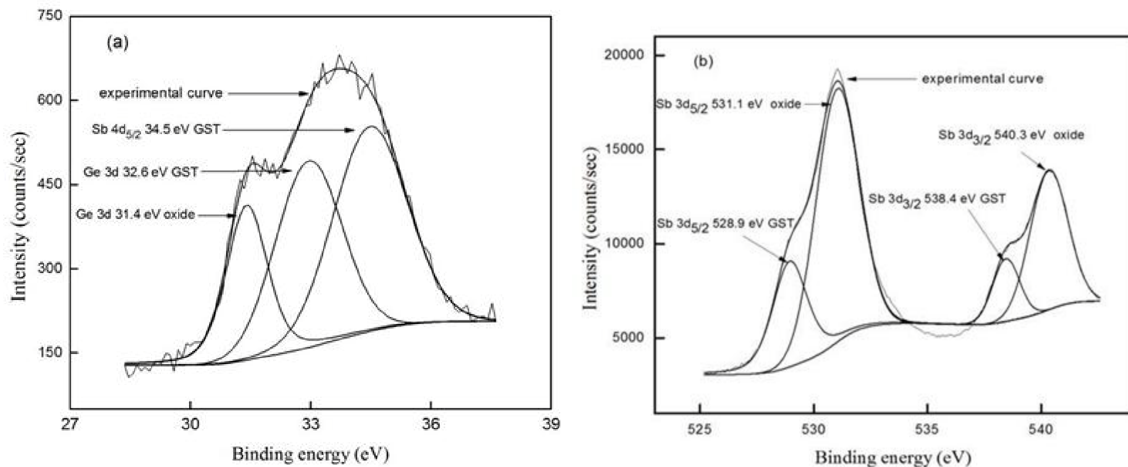

Fig. 2. XPS core level spectra of a photodoped $(Ge_{23}Sb_{23}Te_{54})_{100-x}Ag_{x=2\cdot5}$; (a) Ge 3d, Sb 4d, (b) Sb 3d.

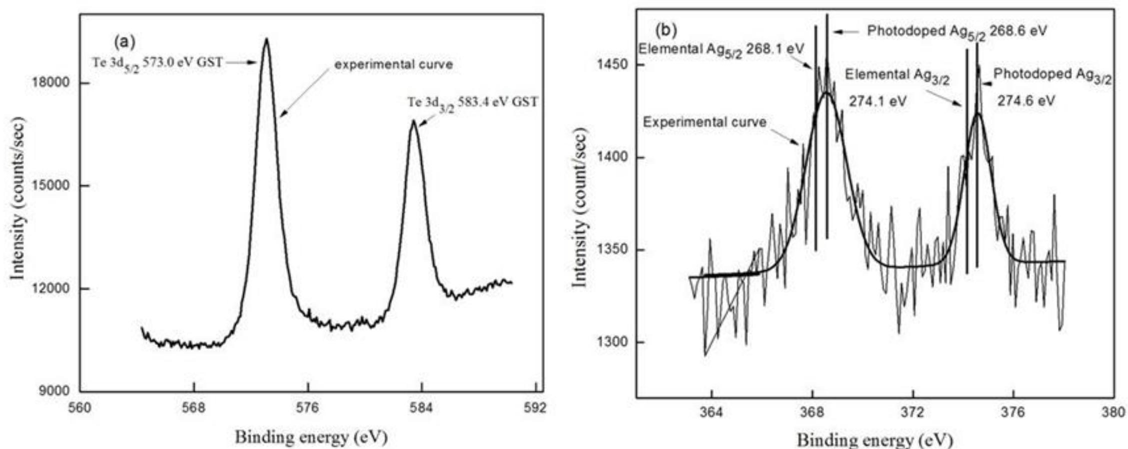

Fig. 3. XPS core level spectra of a photodoped $(Ge_{23}Sb_{23}Te_{54})_{100-x}Ag_{x=2\cdot5}$; (a) Te 3d, (b) Ag 3d.

3.3. *X-ray diffraction*

The structure of annealed films is studied by using x-ray diffraction and sheet resistance measurements. Fig. 4 shows the x-ray diffraction scans of bulk alloy, as deposited film, Ag-photodoped $(Ge_{23}Sb_{23}Te_{54})_{100-x}Ag_{x=2.5}$ film and the annealed films. Absence of any sharp peak for as-deposited $Ge_{23}Sb_{23}Te_{54}$ film confirms the amorphous nature of the film (Curve b). Curve c (Fig. 4) is the x-ray scan of Ag-photodoped $(Ge_{23}Sb_{23}Te_{54})_{100-x}Ag_{x=2.5}$ film illuminated at room temperature and it is clear from the scan that after photodoping of Ag in the $Ge_{23}Sb_{23}Te_{54}$ glassy matrix, the film remain amorphous. This indicates that the Ag uniformly distributed in the matrix without forming cluster. Curve d and curve e (Figure 4) shows, the X-ray diffractograms of annealed $Ge_{23}Sb_{23}Te_{54}$ and Ag-photodoped $(Ge_{23}Sb_{23}Te_{54})_{100-x}Ag_{x=2.5}$ at 210 ^{0}C respectively. Peaks of (102), (103) and (110) planes of hcp structure and peaks of (220), (222) planes of fcc structure of $Ge_2Sb_2Te_5$ (GST) are indentified [16]. Also, the planes of Sb_2Te_3 and GeTe are found in the annealed films. Peaks of (310) and (510) planes of Ag_5Te_3 phase (47-1350, JCPDS database, 1997) are identified in Ag-photodoped $(Ge_{23}Sb_{23}Te_{54})_{100-x}Ag_{x=2.5}$ annealed at 210 ^{0}C.

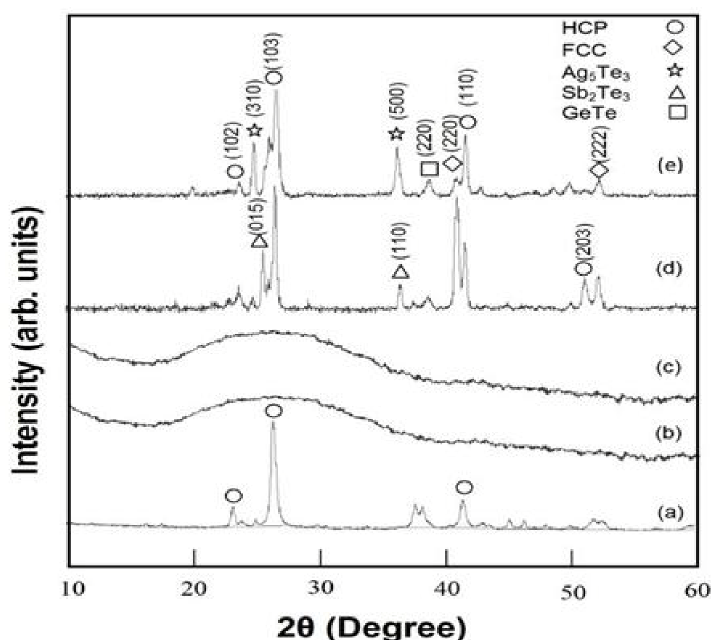

Fig. 4. X-ray diffraction patterns for (a) $Ge_{22}Sb_{22}Te_{56}$ bulk alloy, (b) as deposited $Ge_{23}Sb_{23}Te_{54}$ thin film, (c) photodoped films $(Ge_{23}Sb_{23}Te_{54})_{100-x}Ag_{x=2\cdot5}$ and (d), (e) for $Ge_{23}Sb_{23}Te_{54}$ and photodoped $(Ge_{23}Sb_{23}Te_{54})_{100-x}Ag_{x=2\cdot5}$ films annealed at 210 ^{0}C.

3.4. *Sheet resistance measurements*

Fig. 5 shows the sheet resistance values of $Ge_{23}Sb_{23}Te_{54}$ and photodoped $(Ge_{23}Sb_{23}Te_{54})_{100-x}Ag_{x=2.5}$ films, at a heating rate of 2 ^{o}C/min. A continuous decrease in resistivity is observed followed by an abrupt drop at 125 ^{o}C and 135 ^{o}C for $Ge_{23}Sb_{23}Te_{54}$ and photodoped $(Ge_{23}Sb_{23}Te_{54})_{100-x}Ag_{x=2.5}$ films respectively. For Ag-photodoped $(Ge_{23}Sb_{23}Te_{54})_{100-x}Ag_{x=2.5}$ film amorphous to crystalline phase transformation temperature increases than undoped films this may be due to Ag-Te bond. This may be because the doped Ag atoms substitute for the Ge, Sb, Te atoms or vacancies in $Ge_{23}Sb_{23}Te_{54}$ film, or form compounds with the Ge, Sb, or Te atoms. All the above three reasons will lead to a more stable fcc phase and increase the phase-transition temperature [17]. The presence of the abrupt drop in resistance with temperature is characteristic of Ge-Sb-Te system and indicates that the Ge-Sb-Te system is present as a continuous network in the whole of the sample and is mainly responsible for electrical conduction. The model presented by Kolovov provides a clear explanation of rapid amorphous-crystalline transformation in Ge-Sb-Te system [18]. In $Ge_2Sb_2Te_5$, Te atoms form fcc lattice and Ge occupies octahedral and

tetrahedral positions in the crystalline and amorphous states respectively. At amorphous to crystalline transformation temperature, with the rupture of weak bonds Ge flips into the tetrahedral position. Whereas on melting the Ge atom undergoes a reverse (umbrella) flip to octahedral position resulting in the distortion of the Ge sublattice [19]. This rapid amorphous-crystalline transformation appears as an abrupt drop in resistance in temperature dependent sheet resistance measurements. The reduction in resistance (resistance contrast) upon phase change is more than three orders of magnitude in both cases. The local arrangement of atoms around Sb remains essentially unchanged. The Sb atoms mainly play the role of enhancing overall stability of the metastable crystal structure by participating in the overall electron balance [19].

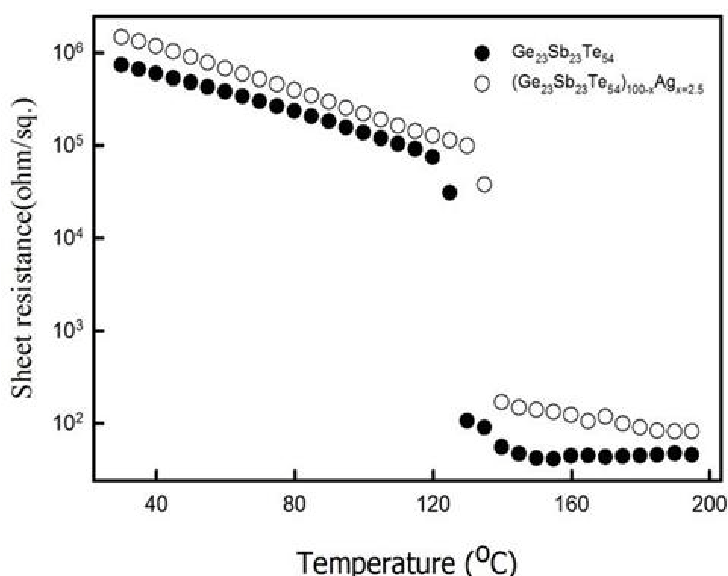

Fig. 5. Sheet resistance variation with temperature for as-deposited $Ge_{23}Sb_{23}Te_{54}$ and photodoped $(Ge_{23}Sb_{23}Te_{54})_{100-x}Ag_{x=2.5}$ films.

4. Conclusions

We have investigated the effect of silver photodoping in the $Ge_{23}Sb_{23}Te_{54}$ amorphous films. Silver after photodiffusion in the glassy matrix may uniformly distributed as the films remains amorphous after silver diffusion and the amount of silver photodoped to be 2.5 at. %. For the XPS analysis it was found that Ag in the glass matrix not in the elementary form rather it forms bond with Te probably Ag_2Te. On annealing both in Ag-photodoped and undoped $Ge_{23}Sb_{23}Te_{54}$ films, mixture of hcp, fcc phases of GST have been identified but the phases of Ag_5Te_3 are formed in Ag-photodoped $(Ge_{23}Sb_{23}Te_{54})_{100-x}Ag_{x=2.5}$ film during crystallization and also, the phase transformation temperature increases for Ag-photodoped film.

Acknowledgements

The authors are grateful to CSIR for the sanctioning of SRF (NET) to one of the authors and for funding a project (03/1140/09/EMR-11). The authors also wish to thank Dr. T. Shripathi (Scientist G) and Mr. U. Deshpande UGC-DAE Consortium for Scientific Research Indore, India for providing access to the XPS facility.

References

[1] R. K. Debnath, A. G. Fitzgerald, K. Christova, Appl. Surf. Sci. **202,** 261 (2002).

[2] M. Kalyva, A. Siokou, S. N. Yannopoulos, T Wagner, Krbal, J. Orava, M. Frumer, J. Appl. Phys. **104,** 043704 (2008).

[3] A. V. Kolobov, S. R. Elliott, Phys. Rev. B **41,** 9913 (1990).

[4] A. V. Kolobov, S. R. Elliott, M. A. Taguirdzhanov, Philos. Mag. B **61,** 859 (1990).

[5] M. T. Kostysin, E. V. Mikhailovskaya, P. F. Romanenko, Sov. Phys. Solid State **8**, 451 (1966).

[6] M. Frumar, T. Wagner, Curr. Opin. Solid State Mater. Sci. **7**, 117 (2003).

[7] V. Weidenhof, I. Friedrich, S. Ziegler, M. Wuttig, J. Appl. Phys. **86,** 5879 (1999).

[8] K. Wang, D. Wamwangi, S. Ziegler, C. Steimer, and M. Wuttig, J. App. Phys. **96**, 5557 (2004)

[9] K. H. Song, S.W. Kim, J.H. Seo, H. Y. Lee, J. Appl. Phys. 104 103516 (2008).

[10] K. Wang, C. Steimer, D. Wamwangi, S. Ziegler, M. Wuttig, Appl. Phys. A **80,** 1611 (2005)

[11] M. Abkowitz, Polym. Eng. Sci. **24**, 1149 (1984).

[12] M. Mitkova, M.N. Kozicki, H.C. Kim, T.L. Alford, Thin solid films **449**, 248 (2004)

[13] A. Kovalskiy, H. Jain, M. Mitkova, J. Non-Cryst.Solids **355**, 1924 (2009).

[14] J. F. Moulder, W. F. Stickle, P. E. Sobol, K. D. Bomben, Handbook of X-ray Photoelectron Spectroscopy, Physical Electronics, Inc., Eden Prairie (1995).

[15] W. S. Lim, S. J. Cho, H. Y. Lee, Thin Sol. Films **516,** 6536 (2008).

[16] W. K. Njoroge, Ph.D thesis, Rheinisch-Westfalischen Technical University, Aachen (2001).

[17] C. T. Lie, P. C. Kuo, W. C. Hsu, T. H. Wu, P. W. Chen, S. C. Chen, Jpn. J. Appl. Phys. **42,** 1026 (2003).

[18] A. V. Kolobov, P. Fons, A. I. Frenkel, A. L. Ankudinov, J. Tominaga, T. Uruga, Nature Mater. **3,** 703 (2004).

[19] A. V. Kolobov, P. Fons, J. Tominaga, A. I. Frenkel, A. L. Ankudinov, S. N. Yannopoulos, K. S. Andrikopoulos, T. Uruga, Jpn J. Appl. Phys. **44,** 3345 (2005).